Research Article   **Open Access**

Andrey E. Krauklis*, Ilo Dreyer

A Simplistic Preliminary Assessment of Ginstling-Brounstein Model for Solid Spherical Particles in the Context of a Diffusion-Controlled Synthesis

Abstract: Wet precipitation (WP) is a diffusion-controlled synthesis method, which is often used for synthesizing such compounds as hydroxyapatite (HAp). Since the process is limited by diffusion, the choice of a diffusion model becomes a critical aspect. In this simplistic assessment for a preliminary evaluation of the diffusion model applicability, the Ginstling-Brounstein (GB) equation is chosen and analyzed for the case of spherical particles. The nominal kinetic constant K is a parameter in GB model which describes diffusion and is related to the effective molecular diffusivity. When the value of K is known, it becomes possible to predict the required time to achieve desired conversion and design the synthesis accordingly. The GB model is assessed mathematically using simulations, a parametric study and Yates analysis (2^n factorial design). Parameters chosen for a preliminary study are in the range of characteristic values for a laboratory-scale WP synthesis of HAp and are thus representative for the application of the model to practice. It should be noted that the analysis is simplistic and is meant to provide only preliminary information for future research, requiring experimental validation.

Keywords: Diffusion-Controlled, Diffusivity, Hydroxyapatite, Biomaterials, Wet Precipitation, Ginstling-Brounstein, Spherical, Mathematical Model, Evaluation, Assessment, Factorial Design, Yates Analysis.

*Corresponding author: Andrey E. Krauklis:** Department of Mechanical and Industrial Engineering, Norwegian University of Science and Technology, 7491 Trondheim, Norway; Institute of General Chemical Engineering, Riga Technical University, Riga, LV-1048, Latvia, E-mail: andrejs.krauklis@ntnu.no
Ilo Dreyer: Institute of General Chemical Engineering, Riga Technical University, Riga, LV-1048, Latvia

1 Introduction

The Ginstling-Brounstein (GB) model is applicable for describing diffusion-controlled processes, and its practical use has been investigated and reported for a wide range of applications [1-18]. Known applications that mention the GB model for describing the kinetics include the hydration of the portland cement particles [1], solid-state synthesis of lanthanum manganite controlled by the three-dimensional solid-ionic diffusion [2], solid-state synthesis of the compound $Zn_{2.5}VMoO_8$ [3], formation of magnesium ferrites [4], dehydration of the iron(III) phosphate dihydrate [5,6], thermal degradation of carbohydrate polymers [7], oxidation and decomposition of three-dimensional braided carbon fibers [8], alkaline hydrolytic decomposition of the uncolored chromium leather wastes [9], thermal stability evaluation of silver sulfathiazole-epoxy resin networks [10], oxidation of boron powder [11], wollastonite fibre dissolution in acetic acid aqueous solution [12], xylan pyrolysis [13], thermal degradation of DGEBA epoxy crosslinked with natural hydroxy acids [14], and pyrolysis mechanisms of lignin-PVA blends [15]. The model has also been applied to some extent in the study of thermal modes of heterogeneous exothermic reactions [16] and the study of inclusion complexes in supramolecular host-guest architectures [17], as well as a methodological study on determination of kinetics from DTA and TG curves [18].

Wet precipitation (WP) is one of the most widely used hydroxyapatite (HAp) synthesis methods and is based on the reaction of calcium hydroxide with the orthophosphoric acid diffusing into the particle. Hydroxyapatite is the main mineral constituent of bones and teeth, and has found its application in various fields such as tissue engineering, orthopedics, prosthetics, drug transport and environmental remediation [19-23]. The orthophosphoric acid is added dropwise into the suspension. The reaction can be written as in the reaction Equation 1.

$$10Ca(OH)_2 + 6H_3PO_4 \rightarrow Ca_{10}(PO_4)_6(OH)_2 + 18H_2O \qquad (1)$$

In this work, the diffusion model is analyzed in the context of diffusion of orthophosphoric acid into the calcium hydroxide particle in a water suspension. However, it has to be noted, that in the studied case, the chemical reaction is much faster than the diffusion, thus, the orthophosphoric acid is diffusing into the reaction product (hydroxyapatite) [24] in reality. The model is somewhat simplified, since it does not account for the presence of byproducts which are normally created in the case of hydroxyapatite synthesis [25].

Another important assumption is that particles can be considered as spherical, which is often only an approximation. The coefficient D is the effective diffusivity. It describes the diffusion in the porous material, and is macroscopic in its nature, e.g., describes not the individual pores, but all the available pores in total [26].

It is related to the molecular diffusivity D_{AB} as shown in Equation 2 [27].

$$D = D_{AB} \frac{\phi \sigma}{\tau}, \tag{2}$$

where τ is tortuosity; ϕ is available porosity; σ is a contraction factor.

The available porosity is equal to the total porosity excluding pores, which are not accessible to the diffusant due to geometrical dimension restrictions, and excluding pores, which are not connected with the rest of the pore system and thus are closed. The contraction factor describes the decrease in the diffusion rate due to the increase of viscosity in the close proximity of pore walls (Renkin's effect) [28,29].

Since the diffusant reacts and diffuses into the particle, the resulting differential equation in the spherical coordinates in the steady state conditions can be written as in Equation 3 [27]. The diffusant's concentration at the particle's surface (r = 0) is C_{AS}.

$$\frac{d^2 C_A}{dr^2} + \frac{2}{r}\left(\frac{dC_A}{dr}\right) - \frac{k_n}{D} C_A^n = 0, \tag{3}$$

where n is the reaction order; k_n is the reaction rate constant.

Solving Equation 3 for the standard boundary conditions, Tile's modulus always appears as shown in Equation 4 [27].

$$\psi = \sqrt{\frac{k_n R^2 C_{AS}^{n-1}}{D}} \tag{4}$$

Based on the Equation 4, it can be deduced that the solution structure does not allow to separately obtain k_n and D, simultaneously, but rather only the ratio. Taking this into account, the simplest model is chosen and is further described. In this work, GB diffusion model is chosen, which is based on earlier Jander's work [30,31].

Diffusion in the spherical particles is a limiting stage in various chemical processes, including the heterogeneous reaction of orthophosphoric acid with the calcium hydroxide. Describing such processes in a general sense, a compound A reacts with a compound B, resulting in a compound AB, whose layer thickness continuously grows during the process. Furthermore, the compound A diffuses into the compound's B surface through the layer of compound AB with such rate that is much lesser than the chemical reaction rate of the A with the B [30].

Since the outer resistance to diffusion is significantly less than the inner resistance of AB, compound's A concentration in the plane dividing A and AB can be considered constant. In the plane dividing AB and B, the concentration of compound A is always equal to zero due to much higher chemical reaction rate between A and B than that of diffusion [30].

As the starting point in GB model a classical diffusion equation for spherical particles is used, represented by Equation 5.

$$\frac{\partial C(r)}{\partial \tau} = D\left(\frac{\partial^2 C(r)}{\partial r^2} + \frac{2}{r}\frac{\partial C(r)}{\partial r}\right) \tag{5}$$

The initial and boundary conditions are shown in Equations 6 - 9.

$$C(r)\Big|_{\substack{r = R \\ \tau > 0}} = C_0 \tag{6}$$

$$C(r)\Big|_{r = R - x} = 0 \tag{7}$$

$$\frac{dx}{d\tau} = \frac{D}{\varepsilon}\left(\frac{\partial C(r)}{\partial r}\right) r = R - x \tag{8}$$

$$x\Big|_{\tau = 0} = 0 \tag{9}$$

where the $\varepsilon = \frac{\rho n}{\mu}$ is the proportionality coefficient when concentration is in the molar units; n is the stoichiometric reaction coefficient which represents compound's A quantity in moles reacting with a single mole of compound's B; μ is compound's A molecular mass.

As one of the solutions intermediate forms to this model the Equation 10 is obtained.

$$x^2\left(1 - \frac{2}{3}\frac{x}{R}\right) = K\tau \tag{10}$$

Equation 10 describes the relationship between the thickness of the reacted layer x and the elapsed time τ. It can be deduced that the rate of the change in layer thickness of compound's AB continuously decreases in time at $\frac{x}{R}$ values from 0 up to 0.5, but then symmetrically increases at $\frac{x}{R}$ values from 0.5 up to 1.

Since it is extremely challenging or even close to impossible to experimentally determine the thickness of the reacted layer in time, Brounstein and Ginstling proposed to use the conversion G in place of x, where G varies from 0 to 1.

In the G − τ coordinates, model can be represented by the Equation 11.

$$1 - \frac{2}{3}G - (1-G)^{\frac{2}{3}} = \frac{K\tau}{R^2} \tag{11}$$

where K is the nominal kinetic constant, and is related to the effective diffusivity as represented by Equation 12.

$$\frac{\sqrt{\pi \varepsilon K}}{2C_0\sqrt{D}} = \frac{exp\left(-\frac{K}{4D}\right)}{\Phi\left(\frac{K}{\sqrt{4D}}\right)} \tag{12}$$

where Φ(y) is the error integral defined as in Equation 13.

$$\Phi(y) = \frac{2}{\sqrt{\pi}}\int_0^y e^{-n^2}du \tag{13}$$

Equation 12 can be solved numerically and the value of D can be obtained. However, in this work, from the practical standpoint, it is more efficient to look into the ways of experimentally evaluating the nominal kinetic constant, since effective diffusivity includes both the diffusivity and reaction kinetic terms, separate evaluation of which is an unnecessary complication in this case and thus to be avoided.

The final GB model is given by Equation 14.

$$1 - \frac{2}{3}G - (1-G)^{\frac{2}{3}} = \frac{K\tau}{R^2} \tag{14}$$

where G is conversion (-); K is nominal kinetic constant (m²/s); τ is time (s); R is particle radius (m).

The nominal kinetic constant K is a parameter in GB model which describes diffusion and is related to the effective molecular diffusivity. When the value of K is known, it becomes possible to predict the required time to achieve the desired conversion and design the synthesis accordingly.

2 Experimental

2.1 Methods

Experiment simulations and analysis methods. The heterogenous reaction occurs at the $Ca(OH)_2$ particle surface. The diffusion model is assessed using the aforementioned GB model. The mathematical model is assessed using experiment simulations. The full output generated during the simulations is available in the Appendix of this work. The particle radius is assumed to be in the range of 0.5 − 1.5 μm. It is known, that in practice it is common for the wet precipitation (WP) synthesis of hydroxyapatite to long for about 5 to 7 hours. It is then reasonable to assume that at this elapsed time the reaction is close to a completion and the conversion can be assumed to be in the range of 0.90 − 0.95. Using the GB model, it is then possible to estimate the value of K.

The experiments are simulated, and the effect of K and R on conversion G is analyzed, as well as the effect of parameters G, R, τ on the value of K in calculations, with the help of statistical methods. 45 simulations were performed in total and are reported in the Appendix of this work. The data is analyzed using 2^n factorial design using Yates Algorithm, also known as Yates Analysis, in order to identify the percentile effect of parameters on the value of K in the model. The model in the form of Equation 12 is used.

Ethical approval: The conducted research is not related to either human or animals use.

3 Results and discussion

3.1 Experimental simulations

Numerical simulations of 18 experiments were performed, that is for the all possible combinations of extreme cases and also a few medium cases for particle radius and elapsed time within the boundaries of the first assumption as represented by the Equation 15. Values chosen for a preliminary study are in characteristic range for a laboratory-scale WP synthesis of HAp.

R = 0.5, 1.0, 1.5 μm
τ = 5, 6, 7 h   (15)
G = 0.90, 0.95

The algorithm of the simulations is as follows: the input parameters (particle radius, conversion and elapsed time) are inserted in the model. The value of K is obtained. Knowing the value of K, and setting G to a value from 0 up to 1 with a step of 0.05, it is then possible to calculate the time required for obtaining the respective conversion.

The results of these 18 simulations (S1 – S18) can be found in the Appendix of this work. The example of the simulation output with the input parameters being R = 1.0 μm, G = 0.9, τ = 7 h is shown in Table 1.

Obtained values of the nominal kinetic constant K are summarized in Figure 1.

As shown in the Figure 1, it can be deduced that the expected value of K is in the range of about $1 \cdot 10^{-19}$ to $3 \cdot 10^{-17}$ m^2/s. It should also be noted, that the larger the R, the larger the scatter of possible K values. Based on the 18 simulations, the results are analyzed via descriptive statistics and the average value of K in the expected range is reported in Table 2. Based on the aforementioned assumption (Equation 15), the expected value of K in the practical conditions of wet precipitation synthesis of hydroxyapatite is $1.14 \cdot 10^{-17} \pm 4.33 \cdot 10^{-18}$ m^2/s (95% probability), which results in 37.87% uncertainty.

3.1.1 Influence of the particle size and nominal kinetic constant on the conversion

Analyzed particle radius influence on the conversion change in time, using the obtained average value of K = $1.14 \cdot 10^{-17}$ m^2/s from the aforementioned 18 simulations (S1 – S18). Additional 6 simulations (R1 – R6) are performed, where the value of K is fixed, and 6 different R values are chosen: 0.5, 1.0, 1.5, 2.0, 2.5, 3.0 μm. Note, that radii higher than 1.5 μm are also used here, in order to obtain more data points and thus a fuller picture of the particle radius influence. Elapsed time in order to reach a specific value of conversion for particles of varying size is shown in Table 3.

Simulations R1 – R6 can be found in the Appendix of this work. The effect of particle radius on the required time to reach the desired conversion is shown in Figure 2.

Looking at the model (Equation 12) and Figure 2, it is obvious that a twofold increase in particle radius results in a fourfold increase in the required elapsed time to reach the same conversion, if all other conditions are unchanged.

The effect of K on the conversion is assessed in the additional 3 simulations (K1 – K3) – in each of these, K is set to a constant value – respectively, in the expected range the minimum, arithmetic mean and the maximum

Table 1: Example of the numerical simulation output.

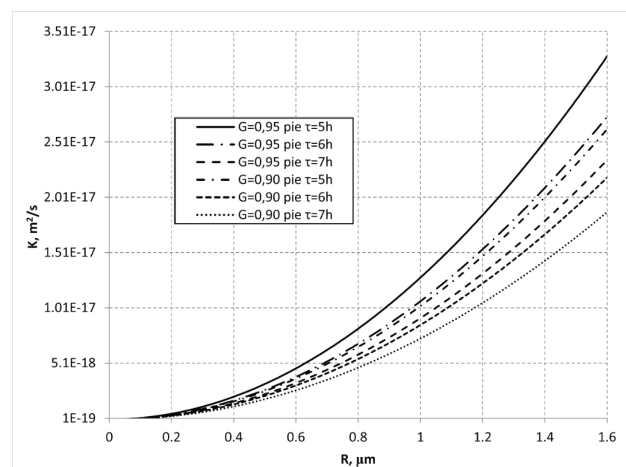| S17		
R =	0.000001	m
G =	0,9	
τ =	7	h
τ =	25200	s
K =	**7.324·10⁻¹⁸**	**m²/s**
1 - (2/3)G - (1-G)^(2/3) = K*τ/R^2		
G	**τ, s**	**τ, h**
0	0	0.00
0.05	39	0.01
0.1	159	0.04
0.15	366	0.10
0.2	668	0.19
0.25	1072	0.30
0.3	1588	0.44
0.35	2225	0.62
0.4	2998	0.83
0.45	3921	1.09
0.5	5012	1.39
0.55	6295	1.75
0.6	7799	2.17
0.65	9561	2.66
0.7	11633	3.23
0.75	14084	3.91
0.8	17023	4.73
0.85	20621	5.73
0.9	25200	7.00
0.95	31534	8.76
1	45515	12.64

Figure 1: Simulation output showing the dependence of K on input parameters G, R and τ.

Table 2: Descriptive statistics results of simulation output K values.

	K, m²/s
Average	$1.143 \cdot 10^{-17}$
Median	$9.709 \cdot 10^{-18}$
Standard Deviation	$8.707 \cdot 10^{-18}$
Excess	-0.877
Skewing	0.579
Scatter Range	$2.704 \cdot 10^{-17}$
Minimum Value	$1.831 \cdot 10^{-18}$
Maximum Value	$2.887 \cdot 10^{-17}$

Table 3: Elapsed time in order to reach a specific value of conversion ($K = 1.143 \cdot 10^{-17}$ m²/s).

R	0.5 µm	1.0 µm	1.5 µm	2.0 µm	2.5 µm	3.0 µm
G	τ, s	τ, s	τ, s	τ, s	τ, s	τ, s
0	0	0	0	0	0	0
0.05	6	25	56	99	155	224
0.1	25	102	229	407	636	916
0.15	59	235	528	938	1466	2112
0.2	107	428	963	1712	2674	3851
0.25	172	687	1545	2747	4291	6180
0.3	254	1017	2288	4067	6355	9151
0.35	356	1425	3207	5701	8907	12826
0.4	480	1920	4320	7680	12000	17280
0.45	628	2511	5650	10044	15694	22599
0.5	803	3210	7223	12840	20063	28890
0.55	1008	4032	9072	16127	25199	36286
0.6	1249	4995	11239	19980	31218	44954
0.65	1531	6124	13778	24494	38272	55112
0.7	1863	7450	16763	29801	46564	67052
0.75	2255	9021	20296	36083	56379	81186
0.8	2726	10903	24531	43611	68142	98125
0.85	3302	13207	29716	52829	82545	118865
0.9	4035	16140	36315	64559	100874	145258
0.95	5049	20197	45442	80787	126229	181770
1	7288	29151	65589	116602	182191	262356

Figure 2: The effect of particle radius on the required time to reach the desired conversion ($K = 1.143 \cdot 10^{-17}$ m²/s).
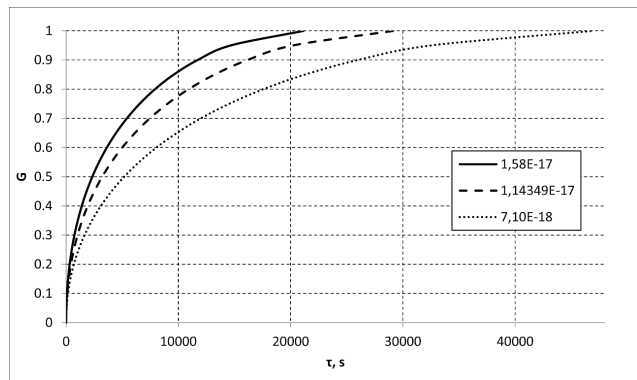
Figure 3: The effect of the nominal kinetic constant on conversion change in time (R = 1 µm).

value is used here, based on the results of the S1 – S18 simulations. In all of these simulations the particle radius is fixed and is 1 µm. Simulations K1 – K3 can be found in the Appendix of this work.

The G = f(τ) relationship is shown in Figure 3, and is a clear representation of how nominal kinetic constant K influences the time required to reach a desired conversion, and is a graphic representation of which is also clear from the model Equation 12. Looking at the model (Equation 12) and Figure 3, it is clear that a twofold increase in nominal
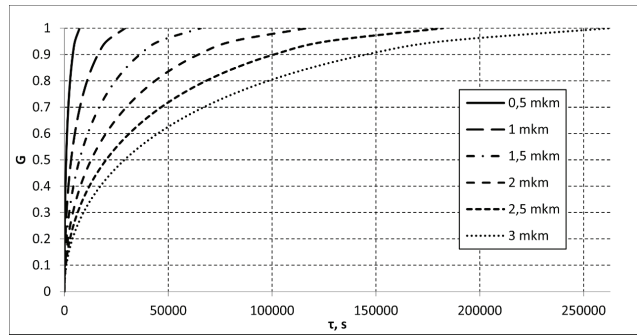
kinetic constant results in a twofold decrease in the required elapsed time to reach the same conversion, if all other conditions are unchanged.

In order to evaluate the mathematical model and to determine the effect of factors R and K on the conversion, the combined analysis is necessary, using descriptive statistics and dispersion analysis ANOVA, two-factor without replication [32].
The analyzed particle radius R and nominal kinetic coefficient K effect on conversion G = 0.90, using results of aforementioned simulations S1 – S18 and of the additional 18 simulations S19 – S36 in order to obtain a fuller picture of the influence. Results of these additional simulations can also be found in the Appendix.

Based on the results of the dispersion analysis shown in Table 6 it is deduced that the percentile effect of factor R is 95.38%, of factor K is only 2.80%, and the error scatter (unexplained dispersion) is 1.82%. However, based on the Fisher's criterion at α = 0.05, the effect of both factors is significant, since $F_R = 105.040 > F_{0.05} = 3.326$ and $F_K = 7.712 > F_{0.05} = 4.103$. Since the effect of both factors R and K is significant and the numbers of residual degrees of freedom

are $\nu_{e,R} = 5 < 10$ and $\nu_{e,K} = 2 < 10$, the dispersion analysis can be stopped here. Based on the analysis it is thus possible to conclude that the effect of the particle size on conversion is significantly larger than that of the nominal kinetic constant. These results indicate that the synthesis time during wet precipitation can be significantly decreased by decreasing the particle size.

3.1.2 Effect of conversion, particle size and time on the nominal kinetic constant value in the model

In the analysis a 2^n factorial design, or Yates Analysis, is used. Complete factorial design (CFD) – a set of multiple

measurements or simulations, which satisfies the following conditions: (1) The number of measurements or simulations is 2^n, where n is the number of factors; (2) Each factor has only 2 values, the lowest and the highest; (3) During the measurement or simulation the lowest and the highest values are combined in all possible combinations. The advantage of such a design is the ease of parameter evaluation [33].

The influence of G, R and τ on the resulting value of K in the model is analyzed. $2^3=8$ simulations are required in order to satisfy the aforementioned condition. The parameter configuration for the respective simulations is reported in Table 7, where „-" and „+" stands for the lowest and highest value, respectively.

Based on the earlier described value range the input parameter values are the following: $R_{min} = 0.5$ μm, $G_{min} = 0.90$, $\tau_{min} = 18000$ s, $R_{max} = 1.5$ μm, $G_{max} = 0.95$, $\tau_{max} = 25200$ s. Additional 8 simulations are performed (FD1 – FD8), based on the model equation in the form of Equation 16.

Results of the simulations can be found in the Appendix of this work. The results of the simulations are shown in the form of a matrix as represented in Table 7 according to the Yates analysis condition.

All 8 combinations and simulations are reported in the specific order as shown in Table 7. All responses are sorted as shown in Table 8. The values of the first column are then calculated – first 4 values are obtained by summing response pairs. For instance, the first value of the first column is the sum of a mean value and the effect's response of R; the second value is obtained by summing G and R·G responses. The last 4 values in the first column are calculated in an analogous fashion, but with the detraction of the responses. For example, the fifth value of the first column is found by detracting response mean from the effect's response of R; the sixth value is found by detracting the G response value from the R·G response.

The second and third column is calculated in the similar manner as the first column, but in the place of responses first and second column values are used, respectively. This algorithm is then continued until the number of numbered columns is the same as the number of factors, which in this case is equal to 3. Values of the

Table 4: Input data for the dispersion analysis.

Gradation classes	K, m²/s, if τ = 5 h	K, m²/s, if τ = 6 h	K, m²/s, if τ = 7 h
R = 0.5 μm	2.563·10⁻¹⁸	2.136·10⁻¹⁸	1.831·10⁻¹⁸
R = 1.0 μm	1.025·10⁻¹⁷	8.544·10⁻¹⁸	7.324·10⁻¹⁸
R = 1.5 μm	2.307·10⁻¹⁷	1.923·10⁻¹⁷	1.648·10⁻¹⁷
R = 2.0 μm	4.101·10⁻¹⁷	3.418·10⁻¹⁷	2.930·10⁻¹⁷
R = 2.5 μm	6.408·10⁻¹⁷	5.340·10⁻¹⁷	4.577·10⁻¹⁷
R = 3.0 μm	9.228·10⁻¹⁷	7.690·10⁻¹⁷	6.591·10⁻¹⁷

Table 5: Dispersion analysis.

	Number	Sum	Mean	Dispersion
R = 0,5 μm	3	6.53·10⁻¹⁸	2.18·10⁻¹⁸	1.35·10⁻³⁷
R = 1,0 μm	3	2.61·10⁻¹⁷	8.71·10⁻¹⁸	2.17·10⁻³⁶
R = 1,5 μm	3	5.88·10⁻¹⁷	1.96·10⁻¹⁷	1.10·10⁻³⁵
R = 2,0 μm	3	1.04·10⁻¹⁶	3.48·10⁻¹⁷	3.46·10⁻³⁵
R = 2,5 μm	3	1.63·10⁻¹⁶	5.44·10⁻¹⁷	8.46·10⁻³⁵
R = 3,0 μm	3	2.35·10⁻¹⁶	7.84·10⁻¹⁷	1.75·10⁻³⁴
K, m²/s, τ = 5 h	6	2.33·10⁻¹⁶	3.89·10⁻¹⁷	1.18·10⁻³³
K, m²/s, τ = 6 h	6	1.94·10⁻¹⁶	3.24·10⁻¹⁷	8.17·10⁻³⁴
K, m²/s, τ = 7 h	6	1.67·10⁻¹⁶	2.78·10⁻¹⁷	6.00·10⁻³⁴

Table 6: The effect of the factors; the results of the dispersion analysis.

Scatter	Sum of Squares	Percentile effect	Degree of Freedom	Dispersion	Fisher's criterion	p–value	$F_{0.05,v,vz}$
Effect of R	1.27·10⁻³²	95.38	5	2.54·10⁻³³	105.040	2.61·10⁻⁸	3.326
Effect of K	3.74·10⁻³⁴	2.80	2	1.87·10⁻³⁴	7.712	0.00941	4.103
Error Scatter	2.42·10⁻³⁴	1.82	10	2.42·10⁻³⁵			
Total	1.33·10⁻³²		17				

effect are then obtained by diving last column's values with the number of simulation, meaning by 8 in this case. If the value is positive or negative, then the correlation sign is „+" and „-", respectively. The values of effect are relative, but they allow to evaluate the percentile effect of parameters on the value o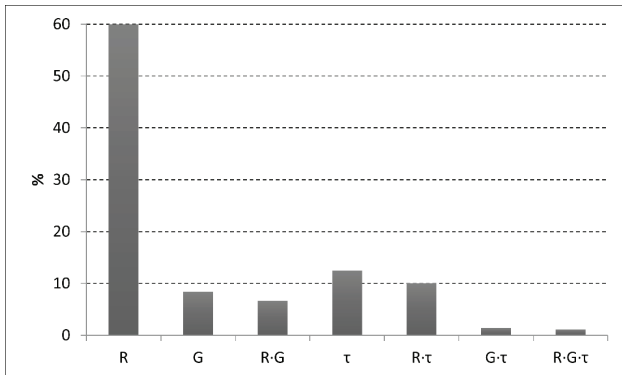f K. Percentile values are then obtained by dividing the modulus of effect values by the modulus of the sum of values [33].

Furthermore, it is possible to evaluate the effect sign; if a sign is „+" or „-", then by increasing the parameter, the response increases or decreases, respectively. It can be concluded that the highest effect on the calculated value of the nominal kinetic constant K is the particle radius R, and is 59.95% as can be seen in Figure 4 and Table 8. The analysis also shows the coupled effect of parameters, which is most significant for the particle radius coupled with time. Thus, in order to obtain K values with a higher precision using the GB model, the highest attention has to be given to the measurements of the particle radius R.

Figure 4: The percentile effect of parameters on the value of K in the model.

Table 7: Input data for the Yates Analysis method.

Simulation	R	G	τ	Response (K)
FD1	-	-	-	$2.563 \cdot 10^{-18}$
FD2	+	-	-	$2.307 \cdot 10^{-17}$
FD3	-	+	-	$3.208 \cdot 10^{-18}$
FD5	+	+	-	$2.887 \cdot 10^{-17}$
FD4	-	-	+	$1.831 \cdot 10^{-18}$
FD7	+	-	+	$1.648 \cdot 10^{-17}$
FD6	-	+	+	$2.291 \cdot 10^{-18}$
FD8	+	+	+	$2.062 \cdot 10^{-17}$

4 Conclusion

In this short and simplistic preliminary study, a mathematical assessment of the Ginstling-Brounstein (GB) model showed that it can be potentially useful in describing the diffusion-controlled synthesis as in the case of wet precipitation (WP) of hydroxyapatite (HAp) using values of the parameters characteristic to the laboratory-scale synthesis of HAp. Particle size determination has the most significant effect (59.95%) on the kinetic coefficient value calculations and thus the highest attention has to be given to the careful measurements of the particle size in order to obtain K values with a high precision. It should also be noted, that reducing particle radius can significantly reduce diffusion-controlled reaction time in order to reach a desired conversion, even operating within the characteristic range of WP parameters in practice, and thus the overall synthesis time can be significantly reduced. An experimental validation of the model will follow.

Table 8: Yates Analysis.

Effect	Response	1st Column	2nd Column	3rd Column	Response Squares	Effect Value	Percentile Effect %	Effect's (correlation) sign
Mean	$2.563 \cdot 10^{-18}$	$2.563 \cdot 10^{-17}$	$5.771 \cdot 10^{-17}$	$9.893 \cdot 10^{-17}$	$6.570 \cdot 10^{-36}$	$1.237 \cdot 10^{-17}$		
R	$2.307 \cdot 10^{-17}$	$3.208 \cdot 10^{-17}$	$4.122 \cdot 10^{-17}$	$7.914 \cdot 10^{-17}$	$5.322 \cdot 10^{-34}$	$9.893 \cdot 10^{-18}$	59.95	+
G	$3.208 \cdot 10^{-18}$	$1.831 \cdot 10^{-17}$	$4.617 \cdot 10^{-17}$	$1.105 \cdot 10^{-17}$	$1.029 \cdot 10^{-35}$	$1.381 \cdot 10^{-18}$	8.37	+
R·G	$2.887 \cdot 10^{-17}$	$2.291 \cdot 10^{-17}$	$3.298 \cdot 10^{-17}$	$8.836 \cdot 10^{-18}$	$8.334 \cdot 10^{-34}$	$1.105 \cdot 10^{-18}$	6.69	+
T	$1.831 \cdot 10^{-18}$	$2.051 \cdot 10^{-17}$	$6.443 \cdot 10^{-18}$	$-1.649 \cdot 10^{-17}$	$3.352 \cdot 10^{-36}$	$-2.061 \cdot 10^{-18}$	12.49	-
R·τ	$1.648 \cdot 10^{-17}$	$2.566 \cdot 10^{-17}$	$4.602 \cdot 10^{-18}$	$-1.319 \cdot 10^{-17}$	$2.715 \cdot 10^{-34}$	$-1.649 \cdot 10^{-18}$	9.99	-
G·τ	$2.291 \cdot 10^{-18}$	$1.465 \cdot 10^{-17}$	$5.154 \cdot 10^{-18}$	$-1.841 \cdot 10^{-18}$	$5.249 \cdot 10^{-36}$	$-2.301 \cdot 10^{-19}$	1.39	-
R·G·τ	$2.062 \cdot 10^{-17}$	$1.833 \cdot 10^{-17}$	$3.682 \cdot 10^{-18}$	$-1.473 \cdot 10^{-18}$	$4.252 \cdot 10^{-34}$	$-1.841 \cdot 10^{-19}$	1.12	-

References

[1] Shi C., Roy D., Krivenko P., Alkali-activated cements and concretes, CRC Press, London, 2005.

[2] Qifeng S., Jiayun Z., Baijun Y., Jianhua L., Phase formation mechanism and kinetics in solid-state synthesis of undoped and calcium-doped lanthanum manganite, Mater. Res. Bull., 2009, 44(3), 649-653.

[3] Tabero P., Bosacka M., Kurzawa M., The reaction mechanism and kinetics of the $Zn_{2.5}VMoO_8$ phase synthesis in the solid state, J. Therm. Anal. Calorim., 2001, 65(3), 865-869.

[4] Paik J.-G., Lee M.-J., Hyun S.-H., Reaction kinetics and formation mechanism of magnesium ferrites, Thermochim. Acta, 2005, 425(1-2), 131-136.

[5] Boonchom B., Puttawong S., Thermodynamics and kinetics of the dehydration reaction of $FePO_4 \cdot 2H_2O$, Physica B: Condens. Matter, 2010, 405(9), 2350-2355.

[6] Khachani M., El Hamidi A., Kacimi M., Halim M., Arsalane S., Kinetic approach of multi-step thermal decomposition processes of iron(III) phosphate dihydrate $FePO_4 \bullet 2H_2O$, Thermochim Acta, 2015, 610, 29-36.

[7] Akbar J., Iqbal M.S., Massey S., Masih R., Kinetics and mechanism of thermal degradation of pentose- and hexose-based carbohydrate polymers, Carbohydr. Polym., 2012, 90(3), 1386-1393.

[8] Gao P., Wang H., Jin Z., Study of oxidation properties and decomposition kinetics of three-dimensional (3-D) braided carbon fiber, Thermochim Acta, 2004, 414(1), 59-63.

[9] Wionczyk B., Apostoluk W., Charewicz W.A., Adamski Z., Recovery of chromium(III) from wastes of uncolored chromium leathers. Part I. Kinetic studies on alkaline hydrolytic decomposition of the wastes, Sep. Purif. Technol., 2011, 81(2), 223-236.

[10] Rosu D., Rosu L., Brebu M., Thermal stability of silver sulfathiazole–epoxy resin network, J. Anal. Appl. Pyrolysis, 2011, 92(1), 10-18.

[11] Jain A., Joseph K., Anthonysamy S., Gupta G.S., Kinetics of oxidation of boron powder, Thermochim Acta, 2011, 514(1-2), 67-73.

[12] Ptáček P., Nosková M., Brandštetr J., Šoukal F., Opravil T., Mechanism and kinetics of wollastonite fibre dissolution in the aqueous solution of acetic acid, Powder Technol., 2011, 206(3), 338-344.

[13] Bar-Gadda R., The kinetics of xylan pyrolysis, Thermochim Acta, 1980, 42(2), 153-163.

[14] Tudorachi N., Mustata F., Curing and thermal degradation of diglycidyl ether of bisphenol A epoxy resin crosslinked with natural hydroxy acids as environmentally friendly hardeners, Arabian J. Chem., (in press), DOI: 10.1016/j.arabjc.2017.07.008.

[15] Corradini E., Pineda E.A.G., Hechenleitner A.A.W., Lignin-poly (vinyl alcohol) blends studied by thermal analysis, Polym. Degrad. Stab., 1999, 66(2), 199-208.

[16] Filimonov V.Yu., Koshelev K.B., Sytnikov A.A., Thermal modes of heterogeneous exothermic reactions. Solid-phase interaction, Combust. Flame, 2017, 185, 93-104.

[17] Varganici C.-D., Marangoci N., Rosu L., Barbu-Mic C., Rosu D., Pinteala M., Simionescu B.C., TGA/DTA–FTIR–MS coupling as analytical tool for confirming inclusion complexes occurrence in supramolecular host–guest architectures, J. Anal. Appl. Pyrolysis, 2015, 115, 132-142.

[18] Blečić D., Živković Ž.D., Martinović M.A, New method for the determination of reaction kinetics from DTA and TG curves. Part I. Definition of the method, Thermochim Acta, 1983, 60, 61-68.

[19] Ozola R., Krauklis A., Burlakovs J., Vincevica-Gaile Z., Rudovica V., Trubaca-Boginska A., Borovikova D., Bhatnagar A., Vircava I., Klavins M., Illite clay modified with hydroxyapatite – innovative perspectives for soil remediation from lead (II), Int. J. Agric. Environ. Res. (IJAER), 2017, 3(2), 177-189.

[20] Sadat-Shojai M., Khorasani M.-T., Dinpanah-Khoshdargi E., Jamshidi A., Synthesis methods for nanosized hydroxyapatite with diverse structures, Acta Biomater., 2013, 9(8), 7591-7621.

[21] Hench L.L., Jones J.R., Biomaterials, artificial organs and tissue engineering, 1st ed., Woodhead Publishing, Cambridge, 2005.

[22] Meski S., Ziani S., Khireddine H., Removal of lead ions by hydroxyapatite prepared from the egg shell, J. Chem. Eng. Data, 2010, 55(9), 3923-3928.

[23] Dong L., Zhu Z., Qiu Y., Zhao J., Removal of lead from aqueous solution by hydroxyapatite/magnetite composite adsorbent, Chem. Eng. J., 2010, 165(3), 827-834.

[24] Kanehira S., Kanamori S., Nagashima K., Saeki T., Visbal H., Fukui T., Hirao K., Controllable hydrogen release via aluminum powder corrosion in calcium hydroxide solutions, JAsCerS, 2013, 1(3), 296-303.

[25] Bērziņa-Cimdiņa L., Dreijers I., Kreicbergs I., Hypothesis of $Ca(OH)_2$ and H_3PO_4 reaction mechanism on solid particle surface, International Forum of Young Researchers "Topical Issues of Subsoil Usage", St. Petersburg, Russia, 2011.

[26] Grathwohl P., Diffusion in natural porous media: contaminant transport, sorption/desorption and dissolution kinetics, Kluwer Academic, Boston, 1998.

[27] Fogler H.S., Elements of chemical reaction engineering, 4th ed., Pearson Education, Westford, 2005.

[28] Renkin E.M., Filtration diffusion and molecular sieving through porous cellulose membranes, J. Gen. Physiol., 1954, 38(2), 225-243.

[29] Thambynayagam R.K.M., The diffusion handbook: applied solutions for engineers, McGraw-Hill Professional, New York, 2011.

[30] Ginstling A.M, Brounstein B.I., О диффузионной кинетике реакций в сферических частицах, Журнал прикладной химии, 1950, 23(12), 1249-1259, (In Russian).

[31] Jander W., Reaktionen im festen Zustande bei höheren Temperaturen. Reaktionsgeschwindigkeiten endotherm verlaufender Umsetzungen, Zeitschr. für anorgan. und allgem. Chem., 1927, 163(1), 1-30, (In German).

[32] Arhipova I., Bāliņa S., Statistika ekonomikā. Risinājumi ar SPSS un Microsoft Excel. Mācību līdzeklis, 2nd ed., Datorzinību Centrs, Rīga, 2006, (In Latvian).

[33] Box G.E.P., Hunter W.G., Hunter J.S., Statistics for experimenters: design, innovation, and discovery, 2nd ed., Wiley, Hoboken, 2005.